ARL-TR-9082 ● SEP 2020

DEVCOM ARMY RESEARCH LABORATORY

Modification and Validation of a Dynamic Indentation Test Apparatus

by John J Pittari III, Jared C Wright, Ryan M Zegarski, and Jeffrey J Swab

NOTICES

Disclaimers

The findings in this report are not to be construed as an official Department of the Army position unless so designated by other authorized documents.

Citation of manufacturer's or trade names does not constitute an official endorsement or approval of the use thereof.

Destroy this report when it is no longer needed. Do not return it to the originator.

ARL-TR-9082 ● SEP 2020

Modification and Validation of a Dynamic Indentation Test Apparatus

John J Pittari III and Jeffrey J Swab
Weapons and Materials Research Directorate, CCDC Army Research Laboratory

Jared C Wright
TKC Global

Ryan M Zegarski
Drexel University, College Qualified Leaders Program

REPORT DOCUMENTATION PAGE

Form Approved
OMB No. 0704-0188

1. REPORT DATE *(DD-MM-YYYY)*	2. REPORT TYPE	3. DATES COVERED (From - To)
September 2020	Technical Report	November 2013–September 2019

4. TITLE AND SUBTITLE
Modification and Validation of a Dynamic Indentation Test Apparatus

5a. CONTRACT NUMBER
W911QX-14-C-0016

5b. GRANT NUMBER

5c. PROGRAM ELEMENT NUMBER

6. AUTHOR(S)
John J Pittari III, Jared C Wright, Ryan M Zegarski, and Jeffrey J Swab

5d. PROJECT NUMBER

5e. TASK NUMBER

5f. WORK UNIT NUMBER

7. PERFORMING ORGANIZATION NAME(S) AND ADDRESS(ES)
CCDC Army Research Laboratory
ATTN: FCDD-RLW-MB
Aberdeen Proving Ground, MD 21005

8. PERFORMING ORGANIZATION REPORT NUMBER
ARL-TR-9082

9. SPONSORING/MONITORING AGENCY NAME(S) AND ADDRESS(ES)

10. SPONSOR/MONITOR'S ACRONYM(S)

11. SPONSOR/MONITOR'S REPORT NUMBER(S)

12. DISTRIBUTION/AVAILABILITY STATEMENT
Approved for public release; distribution is unlimited.

13. SUPPLEMENTARY NOTES
ORCID ID(s): Pittari, 0000-0001-9611-3138; Swab, 0000-0002-8204-7202

14. ABSTRACT

Conventional hardness testing is typically used as a screening metric for material design and performance, especially in the ballistics/armor community, as there is a loose correlation of hardness with armor performance. However, the rate-sensitive behavior of many of these strategic materials is an important factor to consider when designing material systems for impact scenarios. Ergo, the invention of the dynamic indentation hardness tester (DIHT) apparatus was an important development toward measuring the high-rate hardness of these materials. The US Army Combat Capabilities Development Command (CCDC) Army Research Laboratory (ARL) has recently refurbished and redesigned their DIHT unit to include aluminum striker and incident bars, an improved momentum trap assembly, and a redesigned indenter assembly. Background on the original CCDC Army Research Laboratory DIHT and its subsequent redesign and upgrade is included, as well as instructions on the operation of the new indentation apparatus. A preliminary case study was performed to demonstrate that data generated by the ARL DIHT matches literature values. Other performance metrics, aside from hardness, by which this apparatus can be used to capture high-rate performance behavior are also included.

15. SUBJECT TERMS
indentation, high rate, metals, hardness, validation

16. SECURITY CLASSIFICATION OF:			17. LIMITATION OF ABSTRACT	18. NUMBER OF PAGES	19a. NAME OF RESPONSIBLE PERSON
a. REPORT	b. ABSTRACT	c. THIS PAGE			John J Pittari III
Unclassified	Unclassified	Unclassified	UU	28	19b. TELEPHONE NUMBER (Include area code) (410) 306-0773

Standard Form 298 (Rev. 8/98)
Prescribed by ANSI Std. Z39.18

Contents

List of Figures

List of Tables

Acknowledgments

The efforts of Ryan Zegarski, a co-op student from Drexel University, were supported by the Army Educational Outreach Program College Qualified Leaders administered by the Battelle Memorial Institute. The efforts of Jared Wright and the research reported in this presentation were performed in connection with contract/instrument W911QX-14-C-0016 with the Army Research Laboratory (circa 2015). The views and conclusions contained in this document are those of TKC Global and the CCDC Army Research Laboratory. Citation of manufacturer's or trade names does not constitute as official endorsement or approval of the use thereof. The US Government is authorized to reproduce and distribute reprints for Government purposes notwithstanding any copyright notation hereon.

1. Introduction

1.1 Background

Hardness is a quantitative measure of a material's resistance to plastic deformation or, in other words, penetration. Therefore, in general, high-strength brittle materials, which exhibit little to no plastic deformation, tend to possess higher hardness values than ductile materials, which tend to undergo yielding and exhibit plasticity under lower stress states. In the armor community, one of the only properties that has shown any semblance of a correlation to ballistic performance is hardness of the ceramic target,[1–4] or, at a minimum, the difference in hardness between the target and the projectile. Because many modern body armors incorporate a ceramic plate, which are known to exhibit rate-sensitive behavior,[5–13] it is important to understand and consider the properties of the ceramic component as a function of the impact strain rate.

The indentation hardness test is an important tool in any mechanical engineer or material scientist's toolbox. The tests are relatively simple to conduct, further facilitated by the development of modern automated test machines, and have a wide variety of scales by which to quantify the material performance. However, acquiring the dynamic indentation response of materials is not as trivial a task. There have been approaches to acquiring dynamic hardness values using a variety of techniques, such as the rebound method[14–16] or pendulum method[17]; however, these techniques rely on many assumptions and use the velocity of the impactor, rather than directly measuring the load, to determine the hardness. Therefore, their validity has been called into question.[17,18] One of the more common techniques involves using an apparatus based upon the 1-D elastic wave propagation principles of a modified split-Hopkinson pressure bar (SHPB) with a momentum trap assembly.[19,20] The original dynamic indentation hardness tester (DHT or DIHT), from which the US Army Combat Capabilities Development Command (CCDC) Army Research Laboratory (ARL) system is derived, was designed and patented in 2002[21] and is presented in Fig. 1. This technique does not rely on the theoretical formulas in the rebound and pendulum methods, but rather directly measures the indentation load. The size of the resulting indent is measured using a microscope and the hardness is calculated using the conventional equations. This type of system has been used to capture the high-rate indentation hardness value of a variety of materials.[20,2–29]

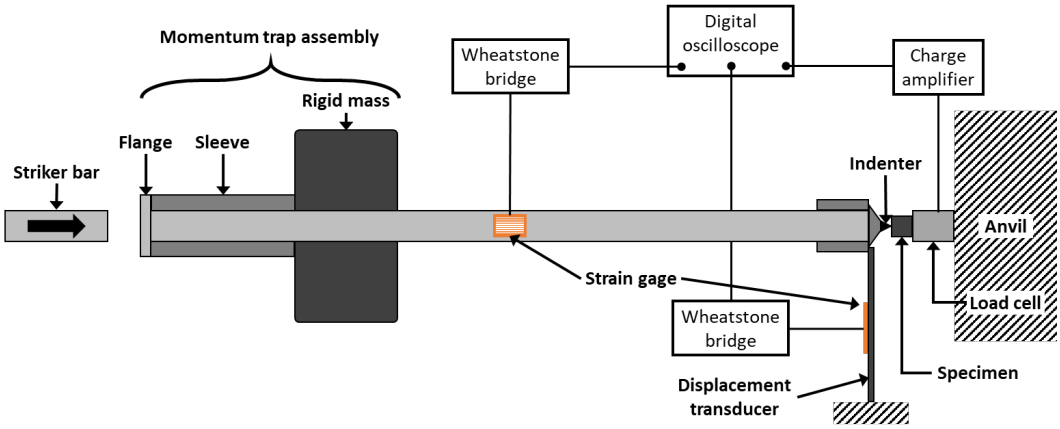

Fig. 1 Schematic of the original dynamic hardness tester

1.2 Basic Operation of the Dynamic Indentation Hardness Tester

The configuration of the DIHT apparatus is similar to the modified SHPB apparatus proposed for recovery compression testing of materials.[19,30] The modification to the original SHPB setup is the addition of the momentum trap assembly, consisting of the flange, sleeve, and rigid mass, to the incident bar. In this instance, the apparatus is further modified by substituting the transmission bar with a high-frequency load cell to determine the indentation force. On the opposite end of the incident bar, an indenter tip is held into an aluminum collar that is attached to the incident bar via set screws, which is what creates the indentation in the specimen. The strain, as a function of time, within the incident bar is recorded by a strain gauge located at the midpoint along the bar length. The specimen is held to the load cell, which is mounted to an anvil with a thin layer of wax, while the indenter tip is placed just out of contact with the specimen surface. This load cell directly measures the load applied to the specimen by the indenter as a function of time, negating the need for a full SHPB-type design. The displacement of the end of the incident bar is measured using a displacement transducer, consisting of a steel strip with one end affixed to the frame of the hardness tester and the other resting on the end of the incident bar close to the indenter. As the indenter is driven into the specimen, the bending of the steel strip is recorded by a strain gauge mounted halfway along the length of the strip.

To initiate a test event, a short striker bar is fired from a gas gun toward the incident bar. Upon impact, a compressive stress pulse is generated within the incident bar, which propagates toward the specimen at a rate equal to the longitudinal wave speed (C_o) of the bar material. Because of the momentum trap assembly, a concurrent compressive stress pulse is generated in the flange-sleeve material,

which travels through the sleeve material toward the rigid mass. As the wave in the sleeve impacts the rigid mass, an equal amplitude wave reflection is generated (i.e., compression to compression) that travels back toward the flange. This wave is now reflecting off a free surface, so it reverses amplitude (i.e., compression to tension) and becomes a trailing (tensile) wave that "chases" the initial compressive wave generated in the incident bar. This results in the compressive wave first reaching the end of the incident bar and causing the indentation event to occur, where the load cell acquires the load signature in the specimen, before reflecting and travelling back along the incident bar as a tensile wave. The trailing tensile wave (from the momentum trap assembly) reaches the end of the incident bar and causes retraction of the bar away from the specimen. The continued traversal and reflection of these waves results in no further indentation events and continued retraction of the incident bar. (For further details of this phenomenon, the reader is referred to Nemat-Nasser et al.[19]) The specimen is then removed from the load cell, and the two diagonal lengths, d_1 and d_2, of the indent impression, as presented in Fig. 2, are measured on a microscope.

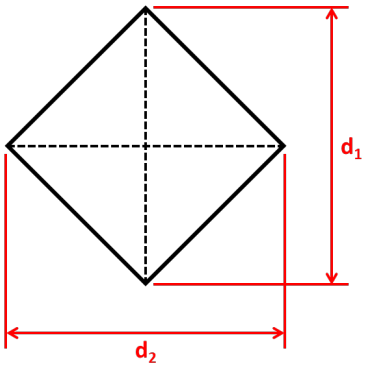

Fig. 2 Schematic of the Vickers indent impression and the corresponding diagonal lengths, d_1 and d_2, that must be measured to perform the hardness calculation in Eq. 1

The Vickers indentation hardness number can now be calculated using Eq. 1, where F is the indentation load in kilogram-force and d is the average indentation diagonal length in millimeters. The coefficient (1.8544) is a standard value based upon the geometry of the Vickers indentation tip. The Vickers hardness number is a dimensionless number.

$$HV = \frac{1.8544 \cdot F}{d^2} \tag{1}$$

Hardness values are commonly presented with units of megapascals (or gigapascals) to facilitate comparison between materials. In this scenario, the indentation force is measured in newtons, resulting in units of newtons per square millimeter, or megapascals, which is the approach used in this study. If a different

indenter type were to be used, then the hardness equation for that specific indenter geometry would also need to be used.

The dynamic indentation process can be very stochastic, especially in comparison to conventional quasi-static testing. For instance, most quasi-static test units can measure the hardness of a material at loads as low as 0.01 kgf or as high at 10 kgf. However, it is typically very difficult to achieve indentation loads below 1 kgf using the dynamic indentation unit due to the difficulty in achieving and maintaining the necessary pressure in the gas gun for these loads. Furthermore, the quasi-static tests are very controllable, and the loads are very repeatable. This is not the case for the dynamic test, where the gas gun pressure, distance between the striker and incident bars, and distance between the indenter tip and specimen can all have an influence on the indentation load. This is further complicated when testing brittle materials, such as ceramics, where cracking and spallation of the indent commonly occur at higher (>2 kgf) loads. In a similar vein, overloading the indenter tip can prove to be problematic. Typical diamond indenters have only a short usable length of diamond available for penetration before the metallic mount material, used to hold the diamond in place in the mount, also begins to penetrate the material, distorting the shape of the resulting indentation. In softer materials, excessive penetration can be a common occurrence. An example of this issue in aluminum can be seen in Fig. 3.

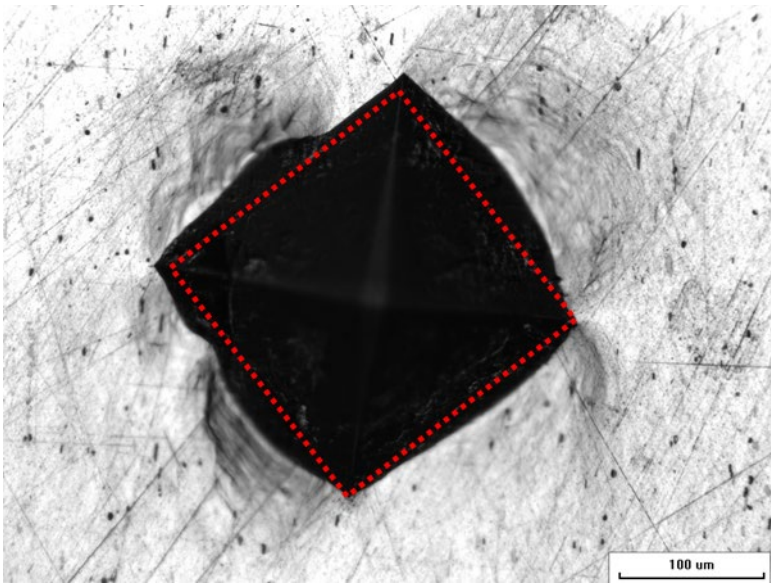

Fig. 3 Excessive penetration of a Vickers indenter tip into aluminum due to a high-load indent (60.5 N), causing distortion of the indent edges as a result of contact with the metallic holder for the diamond tip. The dotted outline indicates the expected indent geometry.

In harder materials, excessive penetration of the indenter tip can often cause damage or break the diamond tip. Lack of proper lubrication and contact between the components of the momentum trap assembly can also cause poor capture and reflections of the waves, which can result in multiple impact events to occur. An example of this issue can be seen in Fig. 4.

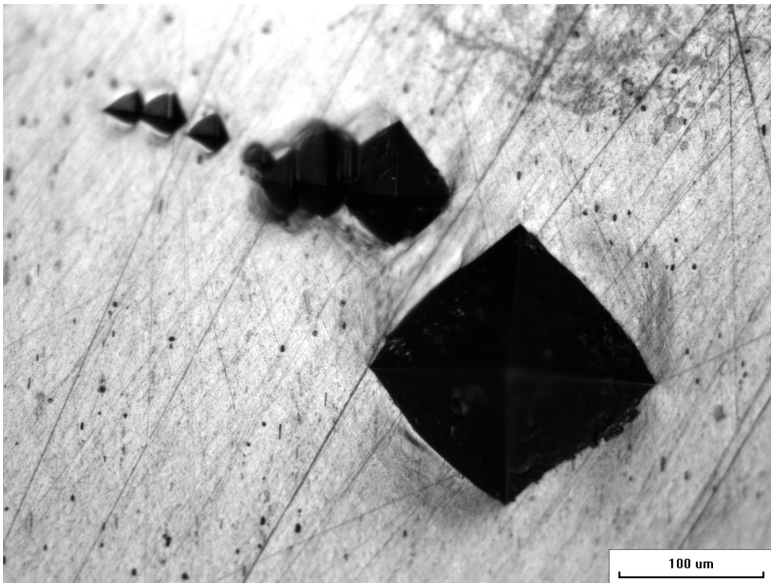

Fig. 4 Multiple indentation events in one test on aluminum due to poor manipulation of the stress waves in the DIHT assembly

The purpose of this study was to redesign the DIHT unit to improve the dynamic indentation process and overcome many of the aforementioned shortfalls with dynamic hardness testing. The new unit would subsequently require validation, hence a case study examination was performed whereby hardness values generated by this refurbished unit were compared to previously reported data on similar materials.[20] Following successful validation, the plan was to employ this redesigned apparatus and methodology to a wide range of material systems for a variety of applications.

2. Design of New DIHT Apparatus

The overall goal of the redesigned DIHT apparatus is to improve the performance and repeatability of the instrument in light of the aforementioned issues with this technique. An overview of the new instrument design can be seen in Fig. 5. The design of the new dynamic hardness tester revolves around four major design changes:

1) New material (aluminum) for the striker and incident bars and the flange and sleeve.

2) Improved momentum trap assembly

3) Reconfiguration of the indenter tip assembly and specimen

4) Removal of extraneous components (steel strip)

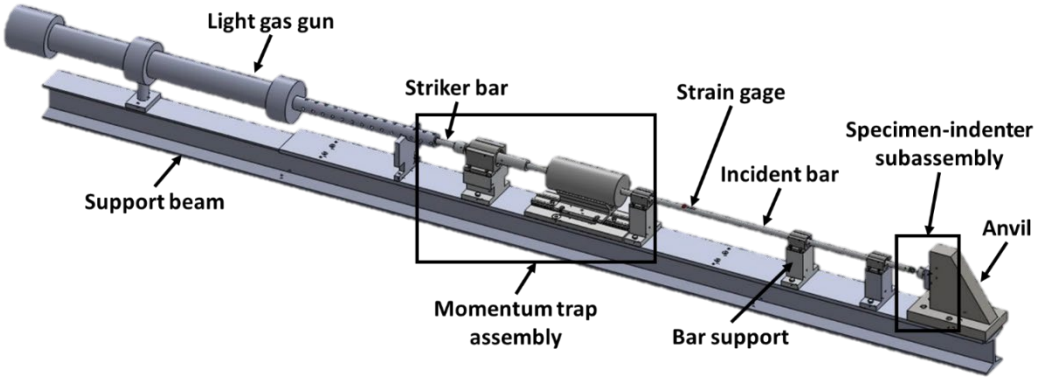

Fig. 5 Solid model design of the new dynamic indentation hardness tester

2.1 New Bar Materials

The first change is the use of aluminum (grade 7075-T6) bars and sleeve in place of the original maraging steel striker and incident bars, as well as the flange and sleeve. The diameter of the incident bar was also increased from 0.375 to 0.5 inches. The material changes do not significantly affect the wave speed in the bar ($C_{Al} \approx C_{Steel}$), but they do decrease the impedance of the bar. These results are presented in Table 1.

Table 1 Comparison of material properties influencing the physics of the original DIHT and the redesigned apparatus

Material	Density (kg/m^3)	Elastic modulus (GPa)	Wavespeed (m/s)	Diameter (mm)	Impedance (Pa-s/m)
Steel	8080	200	4975	9.525	2864
Aluminum	2810	71.7	5051	12.7	1798

The reduction in impedance allows for a more “sensitive” bar, meaning it will promote the ability to make smaller indentations via lower-amplitude incident pulses (i.e., lower-velocity striker bar impact). The reduced density of an aluminum bar also reduces the warpage (i.e., “sagging”) of the bar that can sometimes occur in an SHPB when not in operation.

2.2 Improved Momentum Trap

The second aspect of the redesign is an improved momentum trap assembly. This redesign was accomplished in two steps. The first was the use of a threaded flange, facilitating the exchange of various diameter sleeves. The baseline flange and sleeve were also increased to 1 inch in diameter, significantly increasing the impedance ratio between the sleeve and incident bar. Originally, the impedance ratio between the sleeve and bar was 0.78; however, it has now been increased to 3.0 (Table 2). This helps to ensure that the retraction wave pulses (i.e., "chasing" tensile wave pulses), now having a three times larger amplitude than the compressive wave pulses, appropriately move the incident bar away from the specimen following the initial indentation event, further reducing the occurrence of multiple indentation events.

Table 2 Comparison of the original DIHT sleeve and redesigned sleeve

Material	Sleeve outer diameter (mm)	Sleeve impedance	Impedance ratio (sleeve/bar)
Steel	12.7	2228	0.78
Aluminum	25.4	5394	3.00

The rigid mass has been increased in volume to dramatically increase its ability to act as a rigid surface and improve the functionality of the momentum trap assembly. However, the increased weight of the rigid mass would place undesired stress on the incident bar and its supports, and would eventually cause sagging of the aluminum incident bar over time. To prevent this, the rigid mass is fully supported on linear rollers, ensuring it only contacts the sleeve during operation and never contacts the incident bar. The momentum trap assembly design is shown in Fig. 6.

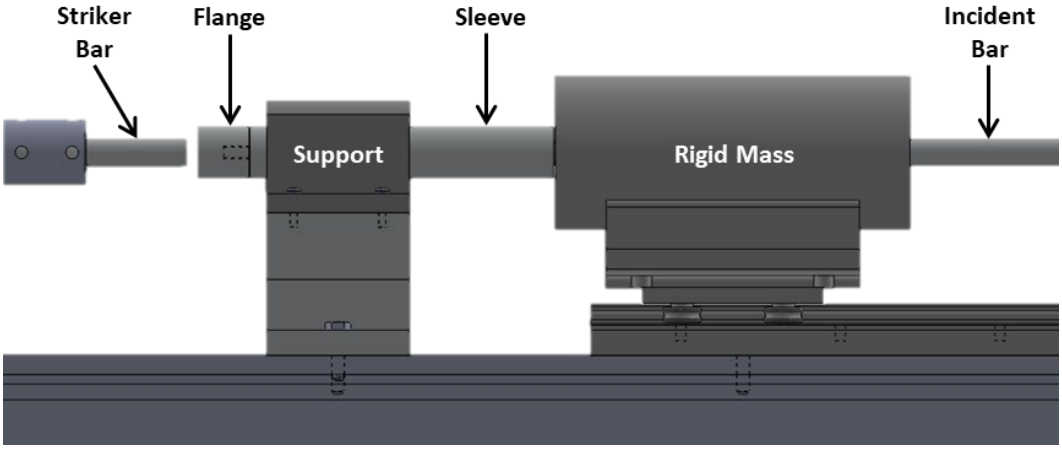

Fig. 6 Detailed schematic of the momentum trap assembly, consisting of the flange, sleeve, and rigid mass

2.3 Configuration of Indenter Tip

The third major design change is in the configuration and mounting of the indenter and specimen. The original design had the indenter tip attached to the incident bar, which was then driven into the stationary specimen during a test. The new design places the specimen on the incident bar and pushes the specimen into the indenter tip, which is in direct contact with the load cell. This configuration is shown in Fig. 7.

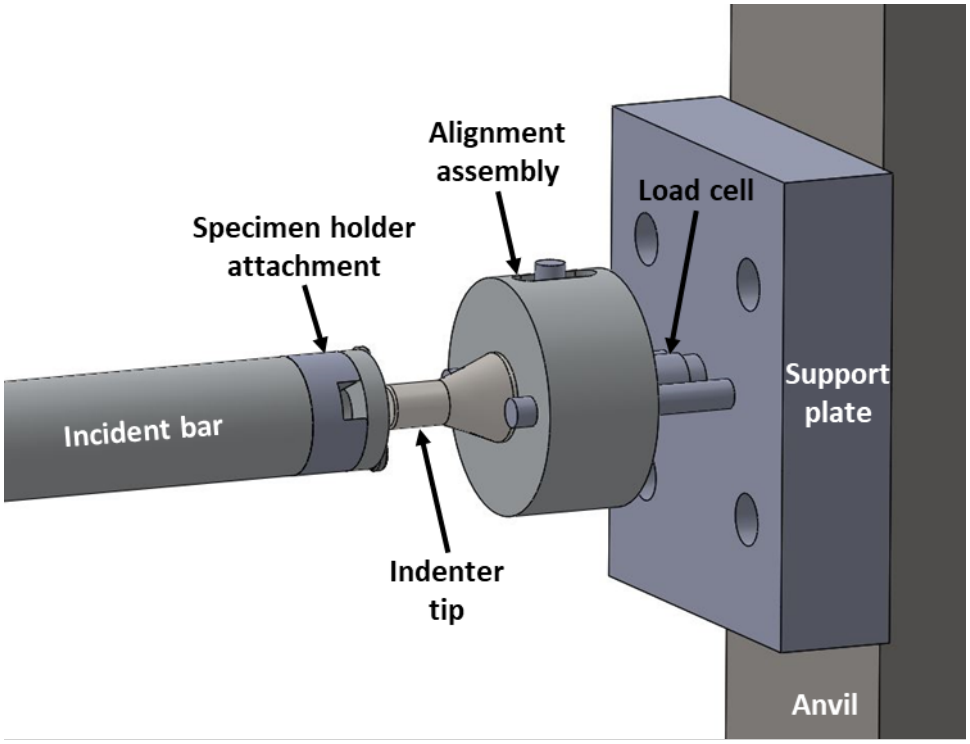

Fig. 7 Larger view of the specimen holder and indenter alignment assembly

The end of the incident bar is also threaded, allowing for different methods of attaching the specimen to the bar. A newly designed accessory allows for a traditional "B" bar specimen (typically used for fracture toughness[31] and flexure testing[32] of ceramics) cross section (3×4 mm^2) to be attached to the incident bar, which is shown in Fig. 7. This facilitates sequential indentation tests on the same specimen through a simple loosen-move-tighten procedure. An additional accessory with a flat face (not pictured) allows for various specimen geometries to be indented via other attachment methods, such as double-stick tape or super glue, similar to the original DIHT design.

2.4 Removal of Extraneous Component

The final aspect of the redesign is the omission of the steel strip used to measure the velocity of the end of the incident bar. The steel strip was originally implemented to measure the displacement rate (i.e., velocity) of the incident bar to determine the exact strain rate for each test. However, the ability of the steel strip to consistently and accurately measure the displacement of the incident bar was questionable. Further, it was deemed unnecessary for operation of the dynamic hardness tester, as the velocity of the incident bar (V_i) can be determined from Eq. 2, relying only on the wave speed in the bar, C_b (material property given in Table 1), and the maximum strain in the incident bar, ε_I (measured from the strain gage on the bar surface). The average strain rate can subsequently be calculated according to Eq. 3, where d is the indent diagonal length.

$$V_i = -C_b \varepsilon_i \tag{2}$$

$$\dot{\varepsilon}_i(t) = \frac{V_i}{d} \tag{3}$$

3. Case Study: Comparison of Vickers Indentation to Literature Data

Due to the design change of the new Dynamic Indentation Hardness Tester, a case study was performed to validate the setup and the data that it produces. The original dynamic indentation hardness tester used by Subhash created dynamic Vickers hardness data for 18 metals.[20] The data for three of these metals (6061 aluminum, Grade 2 "commercially pure" titanium, and Grade 5 titanium, also called Ti-6Al-4V) was used for validation through comparison.

The first step was to machine 3 × 4 × 25 mm^3 specimens ("B" bar cross section) of each material. These specimens were then mounted, and the 4 × 25 mm^2 face was polished following standard metallographic procedures to a 0.25-μm finish to create a smooth surface for indentation, free (or nearly free) of residual stresses. After polishing, quasi-static indentation testing was performed on each material. Ten indentation events were attempted at each of the following loads: 1, 2, 3, 5, 10, 20, 30, and 50 kgf using a Wilson Tukon 2100B hardness testing unit. The indentation load (F) and the average of the two measured indent diagonal lengths (d) were input into Eq. 1 to calculate the quasi-static Vickers indentation hardness values (Table 3).

Table 3 Average quasi-static hardness values for the three metals at each indentation load

Material	Average quasi-static hardness at each indentation load (MPa)							
	1 kgf	2 kgf	3 kgf	5 kgf	10 kgf	20 kgf	30 kgf	50 kgf
6061 aluminum	1040	1036	1034	1034	994	979	1011	1041
Titanium	1677	1700	1705	1680	1641	1593	1625	1637
Ti-6Al-4V	3336	3372	3354	3367	3451	3479	3266	3268

Once quasi-static testing was completed, dynamic testing was conducted for each material. For these tests, the specimens were removed from the epoxy mount following the polishing procedure. The new DIHT apparatus was used to create indents in each specimen until 10 acceptable Vickers indents were acquired. In general, it took approximately 15 to 20 indentation tests to produce 10 acceptable indents. An indent was deemed acceptable if it had straight (or slightly bowed) edges, symmetry between the diagonal lengths (within ±5% of the mean value), and minimal to no cracking, chipping, and spallation. The diagonal lengths were measured using an optical microscope, and the maximum load value was recorded from the load cell signature. These measurements were then used to calculate the dynamic Vickers hardness values using Eq. 1. The values can be found in Table 4.

Table 4 Dynamic indentation hardness values for 10 individual indents on each of the three metals

Material		#1	#2	#3	#4	#5	#6	#7	#8	#9	#10
6061 Al	Load (kgf)	25.3	26.6	28.6	29.2	29.8	31.1	31.8	33.8	37.2	38.6
	DHV (MPa)	1045	1036	1018	1019	1023	1020	1058	1109	993	1032
Ti	Load (kgf)	22.2	25.2	26.2	30.5	31.4	33.1	35.6	35.6	45.5	50.9
	DHV (MPa)	2007	2098	2029	2053	2039	2013	2020	1997	2042	2000
Ti-6Al-4V	Load (kgf)	33.1	42.5	51.1	61.1	64.5	65.6	66.3	66.9	76.0	82.0
	DHV (MPa)	3760	3821	3721	3940	3968	3843	3906	3951	3863	3970

Once all the data had been collected, it was compared to the data from the ASM handbook[20] in an effort to prove the newly redesigned DIHT could reproduce dynamic hardness values. This comparison was done by finding the load-independent hardness for each material, where the slope of the trend line for the plot of indentation load versus square of diagonal length is inserted into Eq. 1 for the term P/d^2 to determine a singular hardness value across the load range for a given material. Conventionally, when a hardness value is presented for a specific material, the load value at which that hardness was obtained is also presented

because some materials show an indentation size effect (i.e., hardness versus indentation load is nonlinear).[33–36] The plots of load versus square of the diagonal length are presented in Fig. 8.

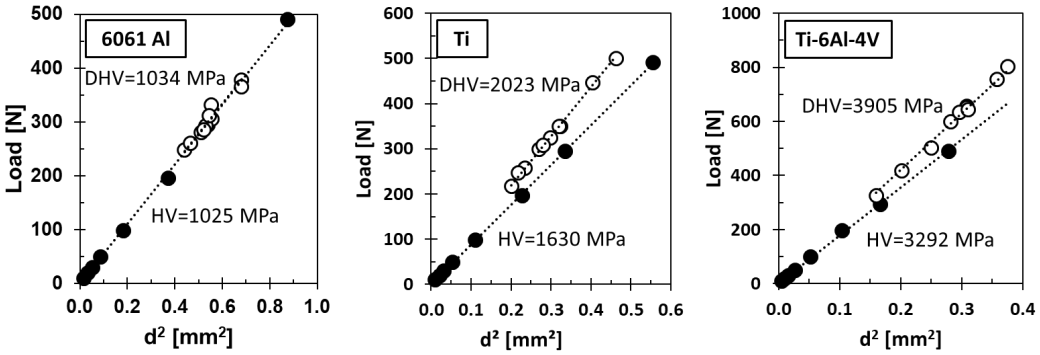

Fig. 8 Plots of indentation load versus square of the diagonal length for the three materials: (left) 6061 aluminum, (middle) titanium, and (right) Ti-6Al-4V. Quasi-static markers are filled, while dynamic markers are empty. The quasi-static markers are an average of 10 indentations at each load, while the dynamic markers represent individual indentation events. The load-independent hardness value is presented for both quasi-static and dynamic loading.

The values derived from this analysis were then compared to the ASM data values[20] to identify any discrepancies. The comparison of quasi-static hardness values is presented in Fig. 9.

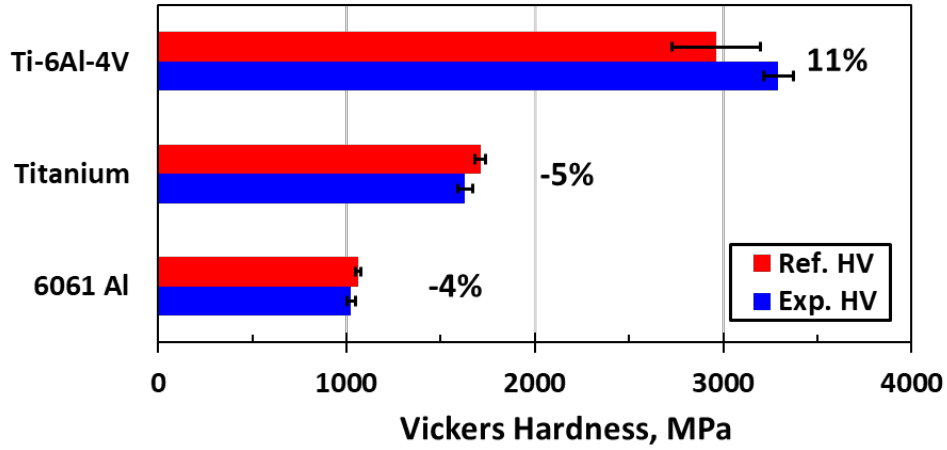

Fig. 9 Comparison of the quasi-static load-independent hardness values from Subhash[20] (red) and the quasi-static hardness values determined from this study (blue). The error bars denote 1 standard deviation.

In general, the percent differences between the current data and the historical data are within ±11%. These differences are likely because the two studies did not test the exact same vintage and microstructure of the various materials. This is especially true of metals, which can undergo many postprocessing procedures to alter the final microstructure of the material. Also, the physical measurement of

indentation diagonal lengths by individual researchers can vary. This can lead to slight inconsistencies in reported hardness values for the same material, generally <6%.[31] A comparison of the dynamic hardness values is presented in Fig. 10. Again, the current values were similar to the previously generated data, falling within ±10% of each other.

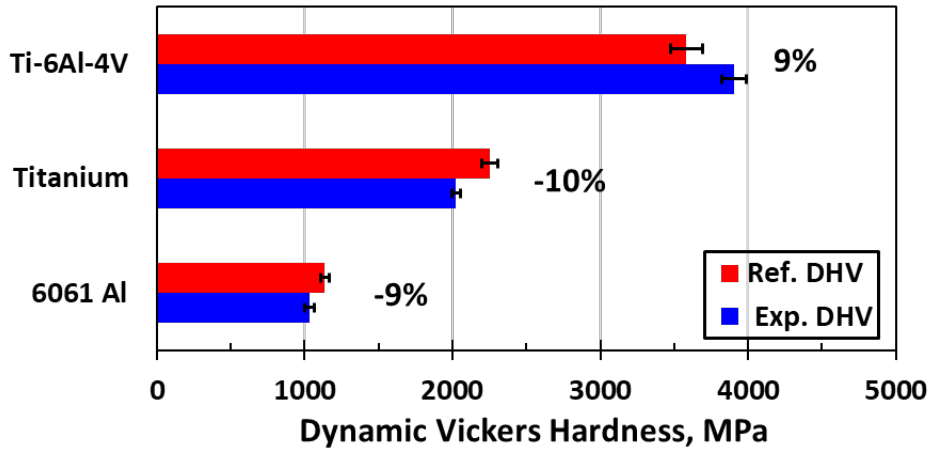

Fig. 10 Comparison of the dynamic Vickers indentation hardness values for the data from Subhash[20] (red) and the experimentally determined values in this study (blue). The error bars denote 1 standard deviation.

The slight variations in hardness values are again attributed to the same considerations made for quasi-static hardness, as the variations are of a very similar degree. This data is plotted in another way in Fig. 11 to compare the percentage increase from quasi-static to dynamic Vickers hardness value for the literature data and the current study's data.

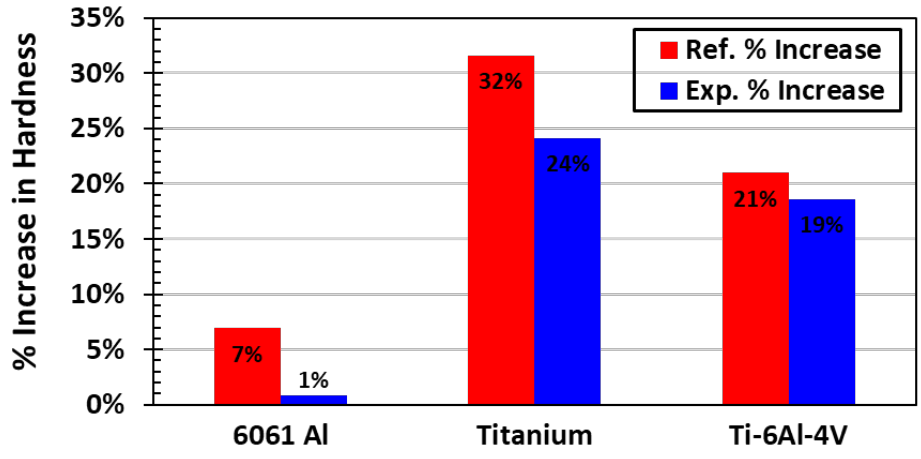

Fig. 11 Comparison of the percentage increase in Vickers hardness from quasi-static to dynamic testing for the data from Subhash[20] (red) and the experimentally determined data from this study (blue)

The crystal structure influences the rate-sensitive behavior of a material due to the various lattices' resistance to deformation and tendency to exhibit different deformation mechanisms under high-rate conditions compared to low-rate. In general, the degree of rate sensitivity increases from face-centered-cubic (FCC) to body-centered-cubic (BCC) to hexagonal-close-packed (HCP) crystal structures during adiabatic deformation.[37] Aluminum has an FCC crystal structure,[38] whose high-rate deformation behavior is dominated by dislocation motion,[37,39] hence it is known to be relatively insensitive to loading rate.[37] This behavior is correctly captured by the redesigned DIHT, where 6061 aluminum exhibits an essentially rate-independent Vickers hardness. The FCC metals investigated in Subhash[20] exhibited a 2%–10% increase in hardness under dynamic conditions, fairly consistent with the results of this study. Titanium is an HCP crystal structure, leading to a high degree of rate sensitivity in the material due to high lattice friction stress (also called Peierls stress) resulting in a propensity to exhibit twinning at high deformation rates.[37,39,40] This high degree of rate sensitivity is again correctly captured by the new DIHT. The titanium alloy Ti-6Al-4V is a mixture of the alpha (HCP crystal structure) and beta (BCC crystal structure) phases,[39,41,42] hence its behavior falling in between the FCC alloy (6061 aluminum) and the HCP metal (titanium). These phenomena are not as pronounced as the historical data demonstrates but are still to a similar degree. Despite some subtle differences in measured hardness values with the data (generally ±11%), the redesigned DIHT shows that it has the ability to produce appropriate dynamic indentation data. With the completion of this case study, future testing and experiments can be completed using this apparatus.

4. Future Directions

The first, and most obvious, extension of this apparatus is the indentation of other classes of materials using various indenter geometries. For example, it is generally recommended to use the Knoop indentation geometry for evaluating ceramic materials due to the reduced indentation depth and stress concentrations associated with this extended pyramid geometry. This geometry results in lower amounts of cracking and spallation in brittle materials, which is a common occurrence with other indenter geometries as the indentation load is increased. There are very few studies presenting the dynamic Knoop hardness values of materials, which would be extremely useful to compare with conventional quasi-static Knoop hardness values.

While the dynamic indentation hardness tester was originally designed to measure the high-rate hardness of materials (as the name implies), it could also prove to be adapted for use in other Army-relevant applications. For example, in ceramic armor materials understanding the nucleation and propagation of cracks is paramount to

achieving high levels of performance. The DIHT apparatus could be modified to investigate the formation and propagation behavior of cracks in ceramic materials, such as the conoid cracks that form in ceramic armor during ballistic impact events[1,43–45] or the propagation of cracks in layered structures, such as ceramic-matrix composites, ceramics produced from highly filled polymer tapes, or layer-by-layer additively manufactured ceramics. The advantage of the DIHT is that a spherical indenter could be used to generate contact cracks from a single impact event, but rather than the impactor continuing to penetrate the material, as in a ballistic test, the impactor is retracted after a small displacement into the specimen, minimizing the surface damage to the specimen and also ending the impact even before full penetration can occur. This could be useful for studying the damage beneath an impact/indent site,[23,46–48] which has been done for quasi-static indentations into silicon carbide at the CCDC Army Research Laboratory.[49]

Another possible adaptation of the DIHT is for small-scale punching experiments. This area is of particular interest to the realm of composites, where understanding the penetration response of a woven fabric is of great concern to performance. Currently, geometric projectiles, simulating the shapes of fragments from an explosive device, are launched from a gas gun into a fabric to capture the deformation response of the composite[50,51]; however, only the overall response of the fabric can be extracted from such tests. The early stages of such an impact event could be captured through calibrated penetration depths of a punch into the fabric.

5. Concluding Remarks

The dynamic indentation hardness of materials has generated great interest in the engineering community, and, further, has great relevance to the high-rate impact situations consistently encountered in Army applications. The DIHT at ARL has been refurbished and redesigned to improve its capabilities and repeatability. Aluminum is now used as the striker and incident bar materials, replacing the previous steel bars, allowing for lower-impact amplitudes. Improvements include a more efficient momentum trap assembly by increasing the size of the sleeve and "floating" the rigid mass on a linear roller bearing. The indenter fixture has been reconfigured to place the specimen directly on the end of the incident bar, and placing the indenter tip into direct contact with the load cell. Preliminary validation of the design shows good agreement with data from three materials (6061 aluminum, titanium, and Ti-6Al-4V) in published literature. Further work will be conducted on other materials (ceramics, glasses, polymers, etc.) and indenter geometries (Knoop, spherical, etc.), and also on other configurations of the apparatus to investigate "recoverable" impact events that probe various deformation behaviors in a variety of materials.

6. References

1. Wilkins ML, Cline C, Honodel CA. Fourth progress report of light armor program. Livermore (CA): Lawrence Livermore National Laboratory; 1969.
2. Wilkins ML, Honodel CA, Sawle D. An approach to the study of light armor. Livermore (CA): Lawrence Livermore National Laboratory; 1967.
3. Wilkins ML, Landingham R, Honodel CA. Fifth progress report of light armor program. Livermore (CA): Lawrence Livermore National Laboratory; 1971.
4. Krell A, Strassburger E. Order of influences on the ballistic resistance of armor ceramics and single crystals. Mater Sci Eng A. 2014;597:422–430.
5. Lankford J. Mechanisms responsible for strain-rate-dependent compressive strength in ceramic materials. J Am Ceram Soc. 1981;64(2):C-33–C-34.
6. Subhash G, Ravichandran G. Mechanical behaviour of a hot pressed aluminum nitride under uniaxial compression. J Mater Sci. 1998;33(7):1933–1939.
7. Suaris W, Shah SP. Rate-sensitive damage theory for brittle solids. J Eng Mechanics. 1984;110(6):985–997.
8. Zinszner J-L, Erzar B, Forquin P. Strain rate sensitivity of the tensile strength of two silicon carbides: experimental evidence and micromechanical modelling. Philos Trans R Soc A. 2017;375(2085):20160167.
9. Meyers MA. Dynamic behavior of materials. John Wiley & Sons; 1994.
10. Subhash G, Nemat-Nasser S. Dynamic stress-induced transformation and texture formation in uniaxial compression of zirconia ceramics. J Am Ceram Soc. 1993;76(1):153–165.
11. Staehler JM, Predebon WM, Pletka BJ, Subhash G. Strain-rate effects in high-purity alumina. Jom. 1995;47(5):60–63.
12. Shih CJ, Nesterenko V, Meyers MA. High-strain-rate deformation and comminution of silicon carbide. J Appl Phys. 1998;83(9):4660–4671.
13. Shih CJ, Meyers MA, Nesterenko VF, Chen SJ. Damage evolution in dynamic deformation of silicon carbide. Acta Materialia. 2000;48(9):2399–2420.
14. Marshall DB, Evans AG, Nisenholz Z. Measurement of dynamic hardness by controlled sharp-projectile impact. J Am Ceram Soc. 1983;66(8):580–585.

15. Sundararajan G, Shewmon P. The use of dynamic impact experiments in the determination of the strain rate sensitivity of metals and alloys. Acta Metallurgica. 1983;31(1):101–109.

16. Tirupataiah Y, Sundararajan G. A dynamic indentation technique for the characterization of the high strain rate plastic flow behaviour of ductile metals and alloys. J Mechanics Phys Solids. 1991;39(2):243–271.

17. Nobre J, Dias A, Gras R. Resistance of a ductile steel surface to spherical normal impact indentation: use of a pendulum machine. Wear. 1997;211(2):226–236.

18. Mok C-H, Duffy J. The dynamic stress-strain relation of metals as determined from impact tests with a hard ball. Int J Mech Sci. 1965;7(5):355–371.

19. Nemat-Nasser S, Isaacs JB, Starrett JE. Hopkinson techniques for dynamic recovery experiments. Proc R Soc A. 1991;435(1894):371–391.

20. Subhash G. Dynamic indentation testing. In: Kuhn H, Medlin D, editors. ASM International; 2000. p. 519–529. (ASM Handbook on Mechanical Testing and Evaluation, vol. 8).

21. Subhash G, Chandra A, Koeppel BJ, inventors; Michigan Technological University, assignee. Apparatus and method for determining the dynamic indentation hardness of materials. Canada Patent CA2207354C. 2004 Sep 28.

22. Klecka MA, Subhash G. Rate-dependent indentation response of structural ceramics. J Am Ceram Soc. 2010;93(8):2377–2383.

23. Ghosh D, Subhash G, Sudarshan TS, Radhakrishnan R, Gao X-L. Dynamic indentation response of fine-grained boron carbide. J Am Ceram Soc. 2007;90(6):1850–1857.

24. Pittari JJ, Subhash G, Trachet A, Zheng J, Halls V, Karandikar P. The rate-dependent response of pressureless-sintered and reaction-bonded silicon carbide-based ceramics. Int J Appl Ceram Tech. 2015;12(S2):E207–E216.

25. Jannotti P, Subhash G, Ifju P, Kreski PK, Varshneya AK. Influence of ultra-high residual compressive stress on the static and dynamic indentation response of a chemically strengthened glass. J Euro Ceram Soc. 2012;32(8):1551–1559.

26. Anton RJ, Subhash G. Dynamic Vickers indentation of brittle materials. Wear. 2000;239(1):27–35.

27. Subhash G, Zhang H. Dynamic indentation response of ZrHf-based bulk metallic glasses. J Mater Res. 2007;22(2):478–485.

28. Haney EJ, Subhash G. Static and dynamic indentation response of basal and prism plane sapphire. J Euro Ceram Soc. 2011;31(9):1713–1721.

29. Hanner LA, Pittari III JJ, Swab JJ. Dynamic hardness of cemented tungsten carbides. IJRMHM. 2018;75:294–298.

30. Nemat-Nasser S. Recovery Hopkinson bar techniques. In: Kuhn H, Medlin D, editors. ASM International; 2000. (ASM Handbook on Mechanical Testing and Evaluation, vol. 8).

31. ASTM C1421 – 10. Standard test methods for determination of fracture toughness of advanced ceramics at ambient temperature. West Conshohocken (PA): ASTM International; 2009.

32. ASTM C1161. Standard test method for flexural strength of advanced ceramics at ambient temperature. West Conshohocken (PA): ASTM International; 2013. p. 1–19.

33. Gane N, Cox J. The micro-hardness of metals at very low loads. Philosophical Magazine. 1970;22(179):0881–0891.

34. Upit G, Varchenya S. The size effect in the hardness of single crystals. In: Westbrook JH, Conrad H, editors. The science of hardness testing and its research applications. Metals Park (OH); American Society for Metals; 1973. p. 135–146.

35. Sargent P, Page T. The influence of microstructure on the microhardness of ceramic materials. Proceedings of the British Ceramic Society; 1978.

36. Clinton D, Morrell R. Hardness testing of ceramic materials. Mater Chem Phys. 1987;17(5):461–473.

37. Gray III GT. High-strain-rate deformation: mechanical behavior and deformation substructures induced. Annual Rev Mater Res. 2012;42: 285–303.

38. Follansbee P. High strain rate deformation in FCC metals and alloys. Los Alamos (NM): Los Alamos National Laboratory; 1985.

39. Gray GT. Influence of strain rate and temperature on the structure. Property behavior of high-purity titanium. Le Journal de Physique IV. 1997;7(C3):C3-423–C3-428.

40. Gray GT. Deformation substructures induced by high-rate deformation. Los Alamos (NM): Los Alamos National Laboratory; 1991.

41. Gooch WA. The design and application of titanium alloys to US Army platforms. Kissimee (FL): International Titanium Association Titanium; 2010.

42. Follansbee P, Gray G. An analysis of the low temperature, low and high strain-rate deformation of Ti−6Al−4V. Metallurgical Trans A. 1989;20(5):863–874.

43. Woodward RL. A simple one-dimensional approach to modelling ceramic composite armour defeat. Int J Impact Eng. 1990;9(4):455–474.

44. Wilkins ML. Mechanics of penetration and perforation. Int J Eng Sci. 1978;16(11):793–807.

45. Woodward RL. Some aspects of cone crack propagation in finite thickness glass plates. Int J Impact Eng. 1988;1(1):1–118.

46. Subhash G, Maiti S, Geubelle PH, Ghosh D. Recent advances in dynamic indentation fracture, impact damage and fragmentation of ceramics. J Am Ceram Soc. 2008;91(9):2777–2791.

47. Gamble EA, Compton BF, Deshpande VS, Evans, AG, Zok FW. Damage development in an armor ceramic under quasi-static indentation. J Am Ceram Soc. 2011;94:s215–s225.

48. Lawn BR. Indentation of ceramics with spheres: a century after Hertz. J Am Ceram Soc. 1998;81(8):1977–1994.

49. Hirsch SG, Walck SD, LaSalvia JC, Swab JJ. Transmission electron microscopy characterization of Knoop indentation inelastic deformation regions in three commercial silicon carbides. Adelphi (MD): Army Research Laboratory (US); 2018. Report No.: ARL-TR-8543.

50. Cheeseman BA, Bogetti TA. Ballistic impact into fabric and compliant composite laminates. Composite Structures. 2003;61(1–2):161–173.

51. Cline J, Moy P, Harris D, Yu J, Wetzel E. Ballistic response of woven kevlar fabric as a function of projectile sharpness. Springer; 2020. p. 13–16. (Dynamic Behavior of Materials, vol. 1).

List of Symbols, Abbreviations, and Acronyms

1-D	one-dimensional
ARL	Army Research Laboratory
BCC	body-centered-cubic
CCDC	US Army Combat Capabilities Development Command
DIHT	dynamic indentation hardness tester
FCC	face-centered-cubic
HCP	hexagonal-close-packed
SHPB	split-Hopkinson pressure bar

1 DEFENSE TECHNICAL
(PDF) INFORMATION CTR
DTIC OCA

1 CCDC ARL
(PDF) FCDD RLD DCI
TECH LIB

2 CCDC ARL
(PDF) FCDD RLW MB
J PITTARI
FCDD RLW ME
J SWAB